Headcut advance modeling in stratified soils
by Dean Allen La Tray

A thesis submitted in partial fulfillment of the requirements for the degree of Master of Science in Environmental Engineering
Montana State University
© Copyright by Dean Allen La Tray (1996)

Abstract:
Headcuts, defined as a natural vertical drop in the bed elevation of an erosive channel, are a significant mechanism of soil erosion. Impinging flow at the overfall concentrates flow energy in a localized area. Headcut development is a transient event, with progressive erosion causing expansion of the scour zone and a concurrent upstream migration of the headcut position. Much past research has focused on modeling headcut formation and movement, but no existing model has been generally tested and accepted. The erosive process is complex, highly variable, and not well understood. A headcut model could be applied to predict earthen spillway damage and to other cases where catastrophic localized scour is of concern.

The current study is designed as a theoretical and experimental investigation of headcut erosion in stratified soils. A two-dimensional, analytic model is constructed and predicts headcut advance rate for the case of a cohesive soil layer overlying a non-cohesive soil base. The model integrates two primary processes: scour hole formation in the base soil and mass failure of the cohesive surface layer. A laboratory-scale physical model is used to test and calibrate the analytical model under ideal, controlled conditions.

Soil mass failure is modeled as a cantilevered beam failing in bending, with soil tensile strength as the limiting parameter for beam stability. Data from beam failure experiments shows decreasing tensile strength with increasing moisture content for the clay used in physical modeling. A modified cantilever model incorporates hydraulic forces acting at the headcut and predicts mass failure length of the surface layer. Applied to flume experiments, the modified analytical model predicted failure lengths with an average error of 25%. This result suggests that the cantilever model successfully represents mass failure in the two-layer soil geometry.

The integrated analytical advance model predicts linear headcut movement with time in a cyclic, self propagating mode. Flume data collected with varying discharge rates and cohesive layer thicknesses show linear headcut movement, supporting the model premise. The analytical model predicted observed rates with an average error of 40% over six data sets. The model development represents a step forward in deterministic headcut characterization and sets a precedent for headcut advance rate predictability in a dual layer geometry, which had not been specifically considered to date.

HEADCUT ADVANCE MODELING

IN STRATIFIED SOILS

by

Dean Allen LaTray

A thesis submitted in partial fulfillment
of the requirements for the degree

of

Master of Science

in

Environmental Engineering

MONTANA STATE UNIVERSITY-BOZEMAN
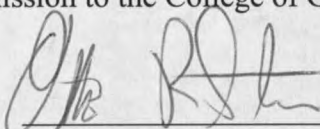Bozeman, Montana

July, 1996

APPROVAL

of a thesis submitted by

Dean Allen LaTray

    This thesis has been read by each member of the thesis committee and has been found to be satisfactory regarding content, English usage, format, citations, bibliographic style, and consistency, and is ready for submission to the College of Graduate Studies.

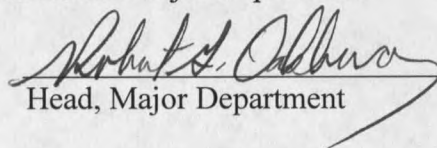Dr. O. R. Stein

               Chairperson, Graduate Committee   17 July 1996
                                                    Date

Approval for the Major Department

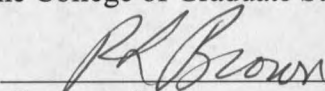Dr. R. G. Oakberg

               Head, Major Department   July 19, 1996
                                                    Date

Approval for the College of Graduate Studies

Dr. R. L. Brown

               Graduate Dean   7/30/96
                                                    Date

STATEMENT OF PERMISSION TO USE

Dean A. LaTray   Date   19 July 1996

TABLE OF CONTENTS

TABLE OF CONTENTS--<u>Continued</u>

LIST OF TABLES

LIST OF FIGURES

LIST OF FIGURES--<u>Continued</u>

ABSTRACT

Headcuts, defined as a natural vertical drop in the bed elevation of an erosive channel, are a significant mechanism of soil erosion. Impinging flow at the overfall concentrates flow energy in a localized area. Headcut development is a transient event, with progressive erosion causing expansion of the scour zone and a concurrent upstream migration of the headcut position. Much past research has focused on modeling headcut formation and movement, but no existing model has been generally tested and accepted. The erosive process is complex, highly variable, and not well understood. A headcut model could be applied to predict earthen spillway damage and to other cases where catastrophic localized scour is of concern.

The current study is designed as a theoretical and experimental investigation of headcut erosion in stratified soils. A two-dimensional, analytic model is constructed and predicts headcut advance rate for the case of a cohesive soil layer overlying a non-cohesive soil base. The model integrates two primary processes: scour hole formation in the base soil and mass failure of the cohesive surface layer. A laboratory-scale physical model is used to test and calibrate the analytical model under ideal, controlled conditions.

Soil mass failure is modeled as a cantilevered beam failing in bending, with soil tensile strength as the limiting parameter for beam stability. Data from beam failure experiments shows decreasing tensile strength with increasing moisture content for the clay used in physical modeling. A modified cantilever model incorporates hydraulic forces acting at the headcut and predicts mass failure length of the surface layer. Applied to flume experiments, the modified analytical model predicted failure lengths with an average error of 25%. This result suggests that the cantilever model successfully represents mass failure in the two-layer soil geometry.

The integrated analytical advance model predicts linear headcut movement with time in a cyclic, self propagating mode. Flume data collected with varying discharge rates and cohesive layer thicknesses show linear headcut movement, supporting the model premise. The analytical model predicted observed rates with an average error of 40% over six data sets. The model development represents a step forward in deterministic headcut characterization and sets a precedent for headcut advance rate predictability in a dual layer geometry, which had not been specifically considered to date.

CHAPTER ONE

1. INTRODUCTION

A headcut, sometimes called a knickpoint, can be defined as a natural, nearly vertical drop in the elevation of a channel bed with erosive boundaries. The drop is a result of concentration of flow energy over a localized area, causing accelerated erosion. In many studied cases, the geometry creating local scour is spatially and temporally constant, such as a bridge pier or cantilevered pipe. In those cases the erosion rate can be quantified in relation to the fixed geometry. However, other instances including gully erosion and breaches of earthen spillways present conditions where erosion is transitory in space and time. Under certain conditions, progressive erosion causes deepening and widening of the scour zone and a concurrent upstream migration of the headcut position. Conditions conducive to transient localized scour can develop quite rapidly, often within a single storm event, and once developed are often self-propagating in that there is a positive feedback between the erosion and the geometry causing the erosion. The scale of this action depends on soil and hydraulic conditions, and can range from millimeters to meters. The mechanism of headcut formation and movement vary greatly.

Headcut erosion models have potential applications in several disciplines. Several headcut researchers have focused on earthen spillway damage, where in extreme cases catastrophic failure could occur. The breaching of clay caps protecting hazardous material,

due to erosion by concentrated channel flow, is another concern. A clay cap breach can cause exposure of protected waste materials and subsequent contamination at down-gradient locations. Other applications include soil erosion prediction and control and geomorphic studies of landscape evolution.

Many research efforts have been made to characterize headcut erosion. Different dominant modes of propagation have been identified in cohesive and noncohesive soils. A large amount of field and physical model data has been collected over the years under various conditions. Several models for headcut movement have been proposed, both empirical and analytical. State-of-the-art erosion models including the Revised Universal Soil Loss Equation (RUSLE) and Water Erosion Prediction Project (WEPP) are not designed to predict soil loss from localized catastrophic scour events. Different models have been used to predict the rate and distance of headcut advance on earthen spillways, but long term validation remains to be done. Due to the complexity of the erosion process and the variability of conditions, none of these models have been generally evaluated and accepted. In general, few studies have attempted to reduce models to component processes and develop them analytically.

The current study is designed as a theoretical and experimental investigation of headcut advance in stratified soils. An existing headcut is presumed; conditions for initiation are not considered. A laboratory-scale physical model was used to create ideal conditions in which critical soil and hydraulic parameters could be controlled. Concurrently, an analytical model was constructed to predict the rate of headcut propagation. The overall goal is to establish a mathematical description of headcut erosion for the specific, well defined

case of a layered soil geometry. This approach was taken to develop a solid analytical framework based on physical data which can then be used as a foundation for further model improvement.

Several specific objectives are currently addressed. First, it was desired to formulate a mathematical model to predict the rate of upstream headcut movement for the case of an erosion resistant, cohesive soil layer overlying a noncohesive soil base. Initial development was to be in two dimensions: longitudinal and vertical. The analytical model would then be tested using a physical model. An essential element of the modeling process is to determine the effects of differing hydraulic and channel bed material properties.

Given the stratified soil geometry, it was necessary to determine the role of soil mass failure as an erosion mechanism. Several researchers have observed mass failure phenomenon, but attempts at analytical quantification have been very limited. It was proposed that a cohesive layer undercut by downstream erosion would fail in bending as a cantilevered slab. Testing the validity of this failure geometry was a fundamental part of model development.

During the course of the study it was found that cohesive tensile strength was a limiting parameter for soil stability. Because tensile strength is not widely documented, a series of experiments was planned to measure the parameter under a geometry very similar to that of the headcut. Experiments were conducted over a range of bulk density and moisture content values.

The body of this thesis is organized as follows. Chapter 2 describes existing headcut models and reviews literature directly relevant to the present study. Chapter 3 details

analytical development of the stratified soil headcut advance model. Different sections describe scour hole formation in noncohesive sand and cantilevered mass failure of the cohesive surface layer. These processes are then integrated to form the final advance model. Chapter 4 details the materials and methods used for physical modeling. Chapter 5 compares the results of the analytical and physical models and discusses model calibration. The final chapter presents conclusions and recommendations for further study.

CHAPTER TWO

2. LITERATURE REVIEW

This review includes first a summary of several research efforts to model headcut movement, beginning with Holland and Pickup in 1976 and concluding with Temple and Moore in 1994. Various approaches have been taken to quantify hydraulic erosive attack and soil and rock resistance to that attack. The large majority of the studies have not broken the erosion process into component elements, but take a broader approach. Often only qualitative observations are provided, based on field or laboratory data. The missing element seems to be research that focuses analytically on specific erosion elements and coordinates the theory with physical data under controlled conditions. This is not to say that the existing models are without merit; in some cases data has been collected for years and much progress has been made in defining the modeling problem.

Secondly, the literature review gives a detailed summary of several research efforts which were used directly in conceptual development of the current headcut model. These studies address jet scour in noncohesive soil and subjects relevant to soil mass failure.

2.1 Holland and Pickup

Holland and Pickup (1976) perform a flume study of knickpoint development in stratified sediment. The study observes headcut formation and movement in three

dimensions. Initial soil geometry consisted of two thin unconsolidated sand layers placed between thicker cohesive layers made of sand and plaster mix. Conclusions include informative qualitative observations on the form and process of headcut movement in stratified soils.

A distinction is made between stepped and rotating headcut morphology. The authors note that stepped knickpoints tend to maintain a vertical face as they move upstream and are characterized by a plunge pool. Stepped headcuts developed as a result of undercutting in the underlying sand layers. When the knickpoints had developed, a channel-in-channel system resulted. In plan view the headcut edge, or lip, tended to be semicircular, and retreat usually occurred when this arcuate form was breached. It was determined that headcut retreat rates generally varied positively in response to changes in discharge. The presence of sand layers stabilized, and generally lowered, erosion rates compared to tests in homogeneous cohesive material. The difference in rates was in some cases more than an order of magnitude.

Holland and Pickup reach a conclusion that sets a precedent for the current research: "...the implications of the present study are that stepped knickpoints developed on knickpoint forming horizons in stratified sediment tend to maintain their form, indicating the presence of an equilibrium condition."

2.2 Begin, Meyer, and Schumm

Begin et al. (1980) develop one of the first analytical models predicting headcut advance rate. Different model forms are presented for rotating and stepped headcut

geometries. Conservation of eroded sediment mass and calculation of downstream sediment transport rate provide a basis for the mathematical development.

The study examines degradation of channels in response to baselevel lowering, accomplished by a discrete drop in flume outlet elevation at time zero during physical data collection. A fundamental tenant of the model combines a sediment continuity equation and a sediment discharge relation to predict channel slope as a function of time and distance from the flow outlet. The differential equation generated is a version of the heat (diffusion) equation, and the solution predicts a decrease in channel slope with both time and distance from the outlet. Sediment discharge is assumed proportional to bed slope, and therefore also decreases accordingly. The authors point out that any chosen sediment discharge relation could be introduced to the model, which could change the channel slope solution.

The geometry used for stepped headcut migration is simple parallel retreat of a vertical headcut face. A sediment mass continuity analysis yields an expression for headcut advance rate:

$$dx/dt = \frac{q_{sd}}{\gamma_s D_h}$$ (2.1)

where: dx/dt = headcut advance rate

$q_{sd}(x,t)$ = downstream sediment discharge rate per unit width

γ_s = bulk sediment weight per unit volume

D_h = headcut height (assumed constant)

The final form of this relation involves substitution for the sediment discharge rate, predicted

to decrease as described earlier. Thus the advance rate decreases proportionally. The authors state that "it becomes increasingly difficult for the channel to cope with the amount of sediments produced in the plunge pool. The expected result is an increased dependance of the velocity of migration of the headcut on the transporting ability of the channel."

The authors collect flume data that indeed shows a decreasing advance rate over time, but this is significantly complicated by factors including channel armoring caused by gravel and coarse sand. The proposed model fits the data only over an initial period of each run presented.

Begin et al. (1980) conclude that the mechanism of downstream transport of sediments supplied by the receding headcut becomes very important. The diffusion model is somewhat qualified by one summary statement: "...the special case of a headcut with a plunge pool at its base represents a most efficient mechanism for disposing of sediments and inducing headcut migration, and it may result in headcut migration with a constant rate."

2.3 Robinson and Hanson

Over the last decade Robinson and Hanson have published several papers examining headcut erosion, focusing on applications to earthen spillways. They present one of the only headcut advance models incorporating a mass wasting component.

In research most relevant to the current work, Robinson and Hanson (1994a) propose a headcut advance model composed of a boundary stress prediction model and a mass failure model. The basic headcut geometry is very similar to that used by Stein and Julien (1993), in which a free-falling nappe is generated at a vertical headcut position. Results of work by

Robinson (1992) determining hydraulic shear stress distribution over an unerodible vertical and horizontal floor below an overfall are incorporated. Resulting sediment detachment is calculated with an excess shear stress equation. A mass failure model based on soil properties and applied forces is developed to characterize the headcut advance. The model geometry assumes shear failure along a Culmann plane passing through the headcut toe. Failure occurs due to undercut and deepening of the overfall face. The length of the failure block is assumed to be equal to half of the overfall height. The model time scale is introduced by the period estimated for erosion of the mass failure material from the scour region.

The authors acknowledge significant simplifying assumptions made in model development. There seem to be some fundamental weaknesses. A Culmann type failure is unlikely to occur in materials with appreciable cohesion, as determined by Thorne (1978). The soil surface in the jet impingement area would not be horizontal, as assumed in the stress distribution calculations. Also, the mechanism used for lag time between failure events seems to poorly represent the physical case. Robinson and Hanson recognize the need for further research and give constructive recommendations on specific points for study. Significant among these is a reliable means of estimating soil erodibility as well as the length and time scales of mass wasting.

Recent Robinson and Hanson publications (1994b, 1994c, 1994d) present results of large scale flume experiments. There is no attempt to apply a deterministic headcut erosion model, although qualitative observations are made on the effects of different physical variables. Advance rates are measured under various conditions, providing valuable data.

The basic setup of the experiments involved compacted soil placed in a large flume (29 m long) in which a pre-formed headcut was constructed. Various overfall heights, discharge rates, degrees of soil compaction and density, and moisture contents were used. Several important points are made. Headcut movement data displayed a typically linear advance with time. Advance rates varied over a large range, from 0.3 to 30 cm/min. Observed rates decreased with higher soil densities and unconfined compressive strength. Different erosion processes were noted, corresponding to the stepped and rotating modes described by other researchers.

A portion of the 1994b study examined the influence of a basal sand layer on headcut advance. The sand effect depended on characteristics of the overlying layer. For highly erodible surface layers the sand had little impact on the headcut advance rate. The overfall in that case typically retreated with a sloping, rather than vertical, face. For overlying material with greater erosion resistance, the sand layer dramatically increased the headcut movement. This finding is an interesting contrast to the earlier observations of Holland and Pickup (1976). Robinson and Hanson (1994b) note that "Classical mass wasting failures were observed as the sand was removed from the base of the overfall, tension cracks formed, and large blocks of soil were removed. The headcut would move upstream with a near vertical face."

2.4 Temple and Moore

Temple and Moore (1994) present a second model for headcut advance, based on a long-term joint study conducted by the Natural Resources Conservation Service (NRCS) and

Agricultural Research Service (ARS). This model also focuses on earth spillway erosion. Headcut advance is predicted using an energy based parameter to quantify the erosive attack and a headcut erodibility index to describe erosive resistance of geologic materials.

A spillway erosion prediction model was developed in three sequential phases: 1) erosion resulting in the local failure of vegetal cover, if any, and development of an area of flow concentration, 2) downward and downstream erosion in the area of flow concentration leading to formation of a vertical or near-vertical headcut, and 3) upstream advance and associated deepening of the headcut. A summary of the third phase is given here. The authors describe this component of the model as the most complex and least understood, resulting in an advance model that is necessarily semi-empirical. Model parameters were calibrated with field data from spillways that had experienced extreme flow events.

The properties of model geologic materials are represented by a headcut erodibility index, K_h. It is a strength based parameter defined as:

$$K_h = M_s(RQD/J_n) J_s (J_r/J_a) \tag{2.2}$$

where: M_s = earth mass strength number

RQD = rock quality designation

J_n = joint set number

J_s = relative ground structure number

J_r = joint roughness number

J_a = joint alteration number

Definitions and discussion on field determination of these terms is given in the appendix to

Temple and Moore (1994). For the case where there were multiple materials in the vertical profile, the depth weighted average of the log of the index for the exposed materials was used. The index range is from 0.01 for cohesionless sand to greater than 10000 for massive, hard rock.

Erosive attack was quantified by use of an energy dissipation term:

$$\dot{E} = q\, \gamma_w\, \Delta H \tag{2.3}$$

where: $\dot{E}$ = flow energy dissipation rate per unit width of headcut

q = volumetric water discharge per unit width

γ_w = unit weight of water

ΔH = change in elevation of the energy grade line through the headcut

A threshold value of this term, $\dot{E}_t$, is defined as the energy dissipation rate associated with headcut erosion causing upstream advance.

The headcut advance rate equation takes the form of an excess attack relation analogous to the excess stress equation used for sediment detachment:

$$dx/dt = C(A - A_o) \quad ; (A - A_o) > 0 \tag{2.4}$$

where: dx/dt = rate of headcut advance upstream

C = material dependant coefficient

A = hydraulic attack

A_o = material dependant threshold attack level below which advance does not occur.

A substitution of terms results in a more definitive form of the equation:

$$dx/dt = C[(q\gamma_w\Delta H)^a - \dot{E}_t^a] \tag{2.5}$$

where a is an empirical constant and all other terms have been previously defined. Both the coefficient C and threshold hydraulic term $\dot{E}_t$ are further presented as functions of the headcut erodibility index. An optimization approach was taken to fit the model to field data by minimizing the summed differences between predicted and observed headcut advance distances. Predicted advance distances were generally consistent with observed values, although considerable data scatter was observed.

In concluding, Temple and Moore state that additional field data and analysis should improve both headcut advance prediction and procedures for determining the erodibility index. They find that data is most scarce for conditions involving high discharges and erosion resistant geologic materials.

2.5 Stein

In his doctoral dissertation (1990) and several later publications (Stein and Julien (1993), Stein et al. (1993), Stein and Julien (1994)), Stein examines and develops model expressions for several aspects of headcut development and migration. The current study is based in large part on the results of his work. The following review summarizes the essential concepts and equations used in this study and referenced in following chapters.

The basic geometry and flow conditions common to Stein's different publications are shown in Fig. 2.1. Steady flow of unit discharge q in two dimensions approaches a headcut
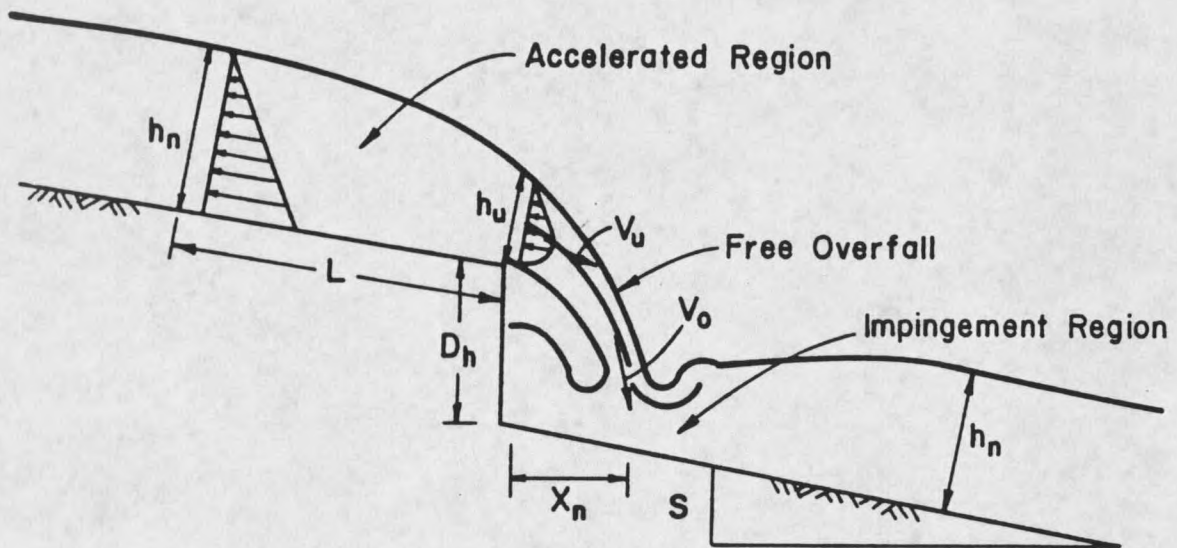
Figure 2.1. Initial Headcut Hydraulics. From Stein and Julien (1993).

over an upstream reach of constant slope. At the overfall a free-falling planar jet forms and impinges obliquely at a point below the headcut. Stein presents a physical analysis based on flow hydraulics and soil characteristics both above and below the headcut position.

2.5.1 Sediment Detachment

An excess shear equation is used for the rate of sediment detachment, as proposed by Foster and Meyer (1975). The sediment detachment rate can be defined as the sediment mass removed from a unit surface area per time:

$$q_s = \kappa (\tau - \tau_c)^\xi \qquad (2.6)$$

where κ and ξ are experimentally determined constants, τ is the applied hydraulic shear stress, and τ_c is the critical shear stress of the bed material. The critical shear stress

represents the threshold where hydrodynamic forces are balanced by gravitational and other resisting forces of a particle on the bed surface. Sediment detachment will occur for any applied shear stress in excess of the critical value. Stein notes that although this equation has a general form, the parameters κ, τ_c, and ξ may all vary significantly under different conditions. Stein et al. (1994) give results for experiments using a fine sand ($d_{50} = 0.15$mm) as follows: $\kappa = 0.30$ s^2/m$^{0.5}$kg$^{0.5}$, $\xi = 1.5$, $\tau_c = 0.35$ Pa. (The units of κ depend on the value of ξ: for $\xi = 1.5$, $\kappa =$ s^2/m$^{0.5}$kg$^{0.5}$. For $\xi = 1.0$, $\kappa =$ s/m.)

The applied hydraulic shear stress is a measure of the friction between a viscous fluid and the flow boundary. This friction is the force causing sediment detachment and creates flow resistance and energy dissipation. Both flow and boundary characteristics affect the magnitude of shear stress. Stein (1990) and Bormann and Julien (1991) translate bed shear stress to a characteristic velocity (V) by using a friction coefficient (C_f).

$$\tau = C_f \rho_w V^2 \tag{2.7}$$

where ρ_w = fluid mass density. For the case of impinging jet flow, the maximum shear stress in the impingement area is determined by the maximum local jet velocity, which can be substituted in the above equation. Bogardi (1974) relates the value of the friction coefficient to the relative roughness of the surface according to:

$$C_f = \frac{\theta_{cr}}{B}(d_{50}/Y_b)^x \tag{2.8}$$

where θ_{cr} is the critical value of the Shield's number, B and x are constants, d_{50} is sediment

size, and Y_b is the diffused jet thickness. Bormann and Julien (1991) give a summary of several research efforts to quantify the parameters B and x, suggesting values of 2.0 - 2.9 for B and 0.19 - 1.20 for x. Both Stein and Bormann use a value of 2.0 for B. In developing an expression for equilibrium scour depth (described in following sections), Bormann shows that the value of the exponent x is of significant importance. The original value used by Bogardi is 0.41, but Bormann found better predictive results with x = 0.5. Bormann suggests that the exponent depends on flow geometry and bed porosity. Stein et al. (1993) successfully use Bormann's results without modification for experiments conducted in two different noncohesive sand sizes.

The critical Shield's number relates to critical shear stress according to:

$$\tau_c = \theta_{cr}(\gamma_s - \gamma_w)d_{50} \tag{2.9}$$

where γ_s = sediment particle specific weight and γ_w = water specific weight. (Note the distinction between particle specific weight and sediment bulk specific weight.)

Stein references the results of Julien and Simons (1985) in relating shear stress to a power function of Reynolds number (Re). The form of the equation depends on the assumption made in calculating the (Darcy-Weisbach) friction factor. The Blasius equation used by Stein is applicable for turbulent flow over a hydrodynamically smooth boundary. The Manning equation applies to turbulent flow over a hydrodynamically rough boundary, and the Chezy equation covers very deep turbulent flow. The Blasius equation gives the Darcy-Weisbach friction factor (f) as:

$$f = 0.22 / Re^{0.25} \tag{2.10}$$

which leads to the friction coefficient employed by Stein, applicable to cohesive soils:

$$C_f = (0.22/8)Re^{-0.25}$$ (2.11)

where $Re = vh_n/v$, v is the average flow velocity, h is flow depth orthogonal to the average velocity, and v is the kinematic viscosity of the fluid.

The sediment detachment rate can be written in terms of sediment continuity as the product of sediment bulk density (B_d) and the change in scour depth (D) with time. Combining this with Eq. 2.6 yields:

$$B_d(dD/dt) = \kappa(\tau - \tau_c)^\xi$$ (2.12)

2.5.2 Upstream and Overfall Flow

Stein (1990) makes a detailed examination of the flow acceleration through the channel reach leading to a free overfall in order to determine the shear stress distribution over that length. For the case where flow detaches for the bed at the brink, atmospheric pressure exists along the lowest streamline. Because of the reduced overfall pressure, flow velocity increases and depth decreases over a short upstream reach to the brink. It is critical to know the overfall flow depth and velocity as these parameters determine the nappe characteristics below the headcut. Stein uses an energy based equation developed by Hager (1983, 1984) to determine these values as a function of upstream flow parameters:

$$V_n/V_u = h_u/h_n = F_r^2/(F_r^2 + 0.4)$$ (2.13)

where V_n and h_n are upstream normal flow velocity and depth, V_u and h_u are brink velocity and depth, and F_r is the flow Froude number. It is noted that this equation is valid only for supercritical flow ($F_r > 1.0$). Given the unit discharge (q), the continuity equation relates discharge, depth, and velocity for both upstream and overfall flow:

$$q = V_n h_n = V_u h_u \qquad (2.14)$$

Julien and Simons (1985) give an equation for upstream normal flow depth as a function of bed slope (S) and flow Reynolds number:

$$h_n = aS^b Re^c \qquad (2.15)$$

where the values of a, b, and c depend on flow and boundary conditions. For turbulent flow over a smooth boundary (Blasius assumption), the coefficients are:

$$a = (0.22v^2/8g)^{1/3}$$

$$b = -1/3$$

$$c = 7/12$$

With the above equations it is possible to calculate flow parameters at the overfall for a given unit discharge and channel slope.

The upstream hydraulic shear stress can also be written as a function of flow depth and channel slope (Stein, 1990):

$$\tau_n = -\rho_w g h_n S \qquad (2.16)$$

where ρ_w = fluid mass density. This basic equation does not account for the flow drawdown in the accelerated reach.

2.5.3 Plunge Pool Hydraulics

As flow passes the overfall, it forms a planar free falling jet which impinges on the initial downstream soil surface at a distance X_n from the headcut face. The flow accelerates through the drop height (D_h), causing the jet thickness to decrease and velocity to increase. At the tailwater impingement point the jet has a thickness Y_0, velocity V_0, and impingement angle χ with the horizontal. Values of jet velocity and thickness at the point of tailwater impingement can be determined from a simple free-falling nappe relationship (Stein and Julien 1994):

$$V_o = (V_u^2 + 2gD_h)^{0.5} \tag{2.17}$$

$$Y_o = q/V_o \tag{2.18}$$

where D_h is the headcut height and g is gravitational acceleration. The jet impingement angle, measured from the horizontal, is given as:

$$\chi = \tan^{-1}[(2gD_h)^{0.5}/V_u] \tag{2.19}$$

Measured horizontally from the headcut face, the impingement point X_n can be located as:

$$X_n = V_u(2D_h/g)^{0.5} \tag{2.20}$$

A plunge pool is rapidly generated in the impingement region as the jet kinetic energy is dissipated by friction at the scour surface, as shown in Fig. 2.2. At a point below the tailwater surface the initial jet entry velocity is reduced as the jet diffuses. Upon approaching the scour surface, the jet streamlines are forced to deflect by the boundary. Flow is directed laterally away from the stagnation point where the jet centerline intersects the unscoured soil surface. Stein (1990) summarizes work done by Beltaos (1972,1974), Kobus et al. (1979), Rajaratnum (1981,1982), Yuen (1984), and Bormann (1988) investigating jet diffusion and impinging jet scour. Much of this work is directed toward characterizing the velocity field resulting from jet diffusion and boundary effects as well as the resulting surface shear forces. The shear stress is generally translated to an equilibrium scour depth. The key to quantifying impinging jet scour is first to determine the characteristic shear velocity in the impingement region and second to determine the particle stability in the scour hole. Both hydraulic and sediment parameters must be considered.

For a distance below the tailwater surface, the jet velocity remains undiminished at V_0. This volume of constant velocity can be defined as the jet potential core, having a length J_p measured from the tailwater entry point along the jet centerline. This length depends only on the jet hydraulic characteristics. For lengths beyond the potential core, the jet velocity decreases. Bormann and Julien (1991) and Stein and Julien (1994) use the following equation to determine jet velocity for centerline lengths $J > J_p$.

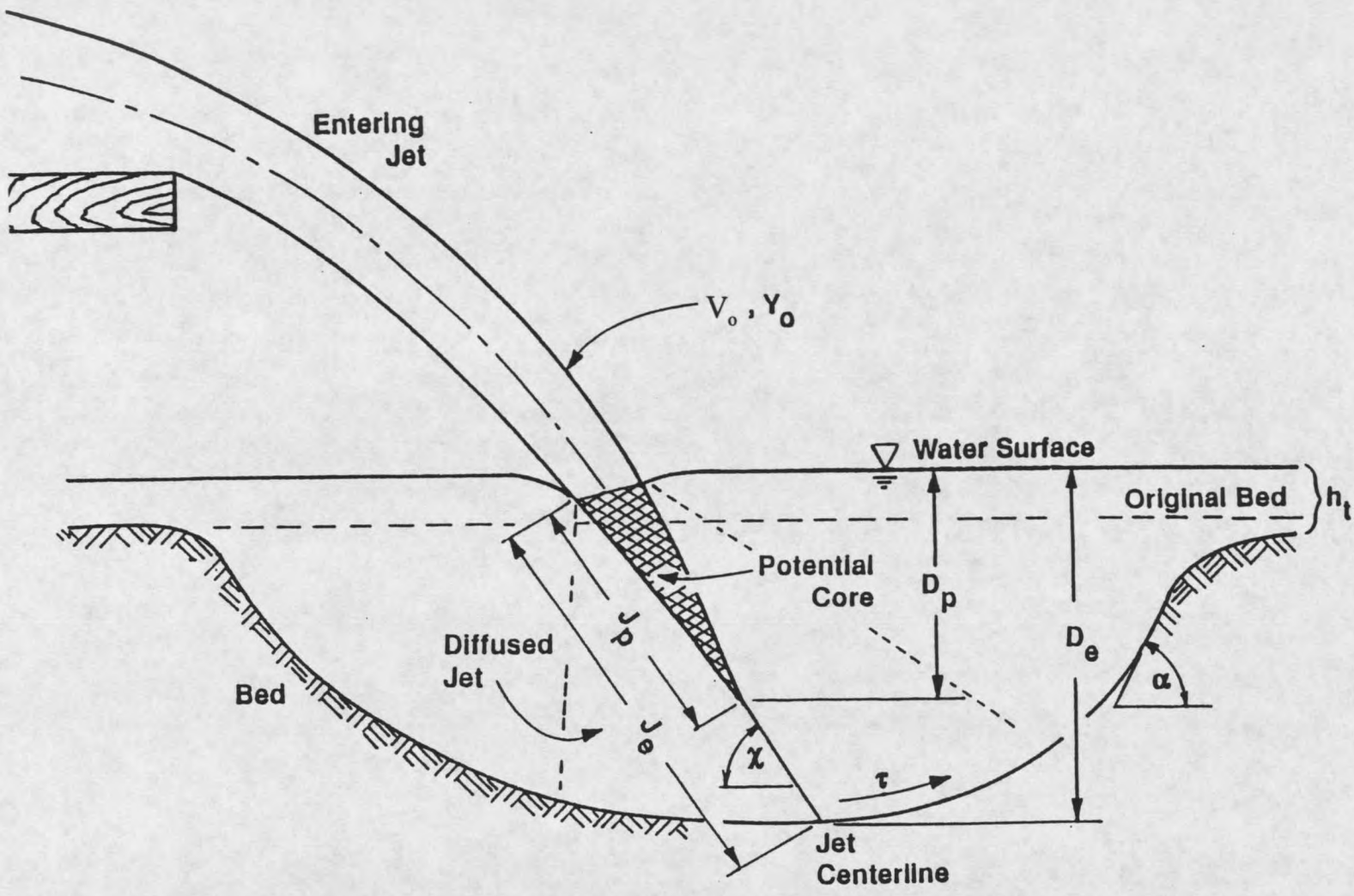$$V/V_o = C_d (Y_o/J)^{0.5} \quad ; J > J_p \tag{2.21}$$

Figure 2.2. Plunge Pool Definition. From Stein and Julien (1994).

Bormann and Julien use this equation to define the velocity near the flow boundary in developing an expression for the equilibrium diffusion length (J_e), described below.

Stein (1990) notes that there is some difficulty in determining the value of the diffusion coefficient (C_d), which can be affected by variations in jet entry velocity, shape of the flow boundary, and the degree of boundary impermeability. Suggested values by Albertson et al. (1950), Beltaos and Rajaratnum (1973), and Yuen (1984), as reported by Bormann and Julien (1991), range from 2.0 to 2.4. Bormann (1988) uses a value of 1.8 while Stein et al. (1993) employ a higher value of 2.6, citing a well formed jet and the influencing factors above. The potential core length can be found by solving the jet diffusion equation for the case that velocity equals the impingement velocity ($V = V_0$):

$$J_p = C_d^2 Y_o \tag{2.22}$$

The vertical depth of scour corresponding to the tip of the potential core can be defined as D_p:

$$D_p = C_d^2 Y_o \sin\chi \tag{2.23}$$

The scour time t_p at which this depth is reached, measured from the moment of initial surface impingement, can be derived as (Stein et al. 1993):

$$t_p = \frac{B_d \, D_p}{\kappa \left(C_f \rho_w V_o^2 - \tau_c \right)^\xi} \tag{2.24}$$

As long as the diffused jet exerts a shear stress in excess of the sediment critical stress, particle detachment will occur and the scour hole will grow in depth and width. Concurrently the jet diffusion length will grow and boundary velocity drops. The scour hole will reach equilibrium proportions when the applied hydraulic forces are balanced by soil particle resistance to detachment. At equilibrium the diffusion length can be defined as J_e and the scour hole depth measured from the original bed level as D_e. The values J_e and D_e are not equal because J_e is measured along the non-vertical jet trajectory.

2.5.4 Equilibrium Scour Depth

Bormann and Julien (1991) derive an equilibrium scour equation based on the concepts of jet diffusion and particle stability in scour holes downstream of grade control structures. Their development considers the results of numerous investigations over a period of 50 years. Results from the developed model are compared favorably to data collected by the authors and several other researchers over a variety of geometries including wall jets, vertical jets, free overfall jets, and submerged jets.

In developing the equilibrium model, Bormann and Julien use Eq. 2.21 to define the diffused jet velocity (V_b) by setting the diffusion length equal to the equilibrium length ($J = J_e$). The continuity equation gives the jet thickness corresponding to the diffused velocity near the soil bed:

$$Y_b = Y_o(V_o/V_b) \qquad (2.25)$$

Bed shear stress and the local friction coefficient (C_f) are given by Eqs. 2.7 and 2.8 respectively. A Shields diagram can be used to find the critical value of the Shields

number in Eq. 2.8. Bormann and Julien translate the critical Shields number to critical

shear stress according to Eq. 2.9.

As reported by Bormann and Julien (1991), a study of forces and moments on

individual particles by Stevens and Simons (1971) examines particle stability on a sloping

bed. The result is an expression for the critical shear stress required to move sediment

particles up on embankment angle α in the direction of flow. The expression is given as

a ratio of the shear stress on a sloping bed (τ_b) to that for a flat bed (τ_{cr}).

$$\tau_b / \tau_{cr} = \sin(\phi + \alpha) / \sin\phi \qquad (2.26)$$

where ϕ = the sediment angle of repose.

Bormann and Julien derive the following expression for the equilibrium

diffusion length J_e.

$$J_e = \left[\frac{\rho_w \sin\phi}{B (\gamma_s - \gamma_w) \sin(\phi + \alpha)} \right]^{2/(2+x)} \frac{C_d^2 \, V_o^{4/(2+x)} \, Y_o^{(2-x)/(2+x)}}{d_{50}^{(2-2x)/(2+x)}} \qquad (2.27)$$

where x is the constant in Eq. 2.8 and all parameters are as previously defined. Bormann

and Julien use x = 0.5 in their study. Substitution yields the final form of the equation.

$$J_e = \left[\frac{\gamma_w \sin\phi}{B g (\gamma_s - \gamma_w) \sin(\phi + \alpha)} \right]^{0.8} \frac{C_d^2 \, V_o^{1.6} \, Y_o^{0.6}}{d_{50}^{0.4}} \qquad (2.28)$$

It is noted that a choice of varying values for the parameter set α, C_d, and B can result in

identical values of J_e.

Bormann and Julien reference a study by Yuen (1984) in assuming that the jet follows a linear trajectory following tailwater entry. For a free jet, this makes the angle of jet intersection with the scour boundary equal to the angle of tailwater entry. This assumption allows calculation of the equilibrium scour depth (D_e) measured from the original bed level.

$$D_e = J_e \sin\chi - h_t \tag{2.29}$$

where χ = tailwater impingement angle, and h_t = tailwater depth. Bormann and Julien point out that ideally a free jet is surrounded by atmospheric pressure as it enters the tailwater. In this case the jet trajectory is not affected by gravity, being neutrally buoyant, or by the Coanda effect. The Coanda effect would exert an influence if pressures were unequal on opposite sides of the jet, such that a vortex was formed on one side. This would be the case for a non-aerated overfall nappe.

2.5.5 Scour Rate

Stein et al. (1993) presents solutions to a differential equation for the rate of vertical scour by an impinging jet. Three equations are given, depending on the value of the exponent of excess shear equation 2.6. Stein suggests an exponent value of 1.5 for non-cohesive sediments, yielding the following expression for the time-depth relation of scour beyond the potential core depth D_p:

$$T^* - T_p^* = \left(D^* - D^{*2}\right)^{0.5}\left(1 - \frac{2}{D^* - 1}\right) - 1.5\arcsin\left(2D^* - 1\right)\Big|_{D_p^*}^{D^*} \quad ; D^* > D_p^* \tag{2.30}$$

All time and depth terms are dimensionless, scaled to the scourhole equilibrium depth D_e and a reference time of no physical significance T_r. D^* is defined as D/D_e, and T^* as T/T_r. T_p^* is the normalized time corresponding to the depth of potential core scour (T_p/T_r). Reference time T_r is defined as:

$$T_r = \frac{B_d D_e}{\kappa \tau_o^\xi} \left(\frac{D_e}{D_p} \right)^\xi = \frac{B_d D_e}{\kappa \tau_c^\xi}$$

(2.31)

Within the potential core, jet velocity and shear stress are constant at V_0 and τ_o. Shear stress can be determined by substituting V_0 in Eq. 2.7. The resulting scour rate is also constant:

$$T^* = D^* \left(\frac{D_p^*}{1 - D_p^*} \right)^\xi \quad ; \quad D^* \le D_p^*$$

(2.32)

Critical shear stress τ_c can be calculated by setting the scour rate equal to zero at equilibrium scour depth:

$$\tau_c = \tau_0 (D_p/D_e)$$

(2.33)

Stein et al. (1993) present model calibration results for experiments with two different sand sizes.

Work by Stein as well as Bormann and Julien summarized in the preceding sections is used as a basis for scour modeling in the current study. The initial headcut geometry presently considered is the same as that used by Stein. Predictive equations for jet velocity